Comparison of ultracentrifugation, density gradient separation, and immunoaffinity capture methods for isolating human colon cancer cell line LIM1863-derived exosomes

Bow J. Tauro [a,b], David W. Greening [a], Rommel A. Mathias [a], Hong Ji [a], Suresh Mathivanan [a], Andrew M. Scott [c], Richard J. Simpson [a,*]

[a] Department of Biochemistry, La Trobe Institute for Molecular Science, La Trobe University, Bundoora, Victoria, Australia
[b] Department of Biochemistry and Molecular Biology, The University of Melbourne, Parkville, Victoria, Australia
[c] Ludwig Institute for Cancer Research, Austin Hospital, Heidelberg, Victoria, Australia

ARTICLE INFO

ABSTRACT

Exosomes are 40–100 nm extracellular vesicles that are released from a multitude of cell types, and perform diverse cellular functions including intercellular communication, antigen presentation, and transfer of oncogenic proteins as well as mRNA and miRNA. Exosomes have been purified from biological fluids and in vitro cell cultures using a variety of strategies and techniques. However, all preparations invariably contain varying proportions of other membranous vesicles that co-purify with exosomes such as shed microvesicles and apoptotic blebs. Using the colorectal cancer cell line LIM1863 as a cell model, in this study we performed a comprehensive evaluation of current methods used for exosome isolation including ultracentrifugation (UC-Exos), OptiPrep™ density-based separation (DG-Exos), and immunoaffinity capture using anti-EpCAM coated magnetic beads (IAC-Exos). Notably, all isolations contained 40–100 nm vesicles, and were positive for exosome markers (Alix, TSG101, HSP70) based on electron microscopy and Western blotting. We employed a proteomic approach to profile the protein composition of exosomes, and label-free spectral counting to evaluate the effectiveness of each method. Based on the number of MS/MS spectra identified for exosome markers and proteins associated with their biogenesis, trafficking, and release, we found IAC-Exos to be the most effective method to isolate exosomes. For example, Alix, TSG101, CD9 and CD81 were significantly higher (at least 2-fold) in IAC-Exos, compared to UG-Exos and DG-Exos. Application of immunoaffinity capture has enabled the identification of proteins including the ESCRT-III component VPS32C/CHMP4C, and the SNARE synaptobrevin 2 (VAMP2) in exosomes for the first time. Additionally, several cancer-related proteins were identified in IAC-Exos including various ephrins (EFNB1, EFNB2) and Eph receptors (EPHA2–8, EPHB1–4), and components involved in Wnt (CTNNB1, TNIK) and Ras (CRK, GRB2) signalling.

1. Introduction

Exosomes are a discrete population of small (40–100 nm diameter) membranous vesicles that are released into the extracellular space from multivesicular bodies (MVBs) by most cell types [1,2]. Typically, the monitoring of exosome isolation has been based upon their size, morphology, flotation density and the presence of marker proteins such as Alix, TSG101, HSP70 and CD9 [1]. Recently, it has been shown that exosomes are also present in body fluids such as synovial fluid [3], saliva [4], urine [5], semen [6], breast milk [7] and, importantly, blood [8]. Originally, exosomes were implicated in the mechanism for removal of cell surface molecules in reticulocytes [9–11] followed shortly thereafter as possible vehicles for antigen presentation [12,13] and immune suppression in cancer [14,15]. More recently, exosomes have

gained much attention for their important role in intercellular communication [16–18]. For example, exosomes have been reported to provide a mechanism for generating soluble cytokine receptors via protease-dependent [19] or protease-independent receptor ectodomain cleavage [20]. In a seminal study, cancer cell derived-microvesicles containing oncogenic proteins (e.g., the truncated, oncogenic form of EGFRv111) – referred to as 'oncosomes' – have been shown to traverse the tumour microenvironment and be taken up by recipient EGFv111 receptor null cells leading to transfer of oncogenic activity [21]. Additionally, cancer-derived exosomes have been reported to contain tumour progression related proteins such as L1CAM, CD24, ADAM10, and EMMPRIN [22] and amphiregulin [23]. Moreover, they have also been shown to initiate proangiogenic signalling cascades in melanoma cells [24]. In addition to proteins, exosomes have also been shown to be carriers of endogenous mRNAs and miRNAs [25,26] and lipid mediators [27], which can modulate the translational activity of recipient cells. Clinically, there is growing interest in the potential use of exosomes as disease biomarkers (e.g., miRNA signatures from disease-derived exosomes circulating in blood [28]), vaccine candidates for tumour immunotherapy [29] (for reviews, see [30,31]), gene delivery vehicles (e.g., siRNA carriers [32]; for a review/commentary, see [33,34]) and as mediators of myocardial ischaemia/reperfusion injury [35]. Despite recent advances in our understanding of exosome biology, much of this information has been obtained from impure exosome preparations, which have confounded interpretation of findings. For example, it is well known that eukaryotic cells release many membranous particle types into the microenvironment, these include exosomes, exosome-like microparticles, shedding microvesicles (SMVs), apoptotic blebs (ABs) [18] and the recently described 'gesicles' [36]. Hence, there is an urgent need to better define exosome preparations so that information obtained at both protein and RNA levels can be appropriately interpreted with respect to unambiguous biological function. Likewise, it is important to accurately define homogeneous exosome populations before embarking on large-scale production for the purpose of detailed biochemical analyses and/or preparation of clinical-grade reagents.

It is well recognised that cell culture media contain, in addition to cell detritus, several types of released membranous vesicles [18]. Thus, it is important to work with as pure a sample as possible, especially when undertaking functional exosome studies. Current strategies for purifying and characterising exosomes from cell culture medium or body fluids differ significantly. In the original and widely-used method for purifying exosomes from culture media [37], differential ultracentrifugation was employed to first remove intact cells and bulky cell debris by low g force centrifugation (e.g., 500g, 2000g) followed by high g force (e.g., 100,000g) to sediment exosomes. In some strategies, the initial low speed centrifugation step(s) has been replaced by 0.1 μm [38] or 0.22 μm [39] filtration or inclusion of an intermediate g force centrifugation step (e.g., 60,000g) to remove shed microvesicles (500–2000 nm diameter) [40]. In order to purify exosomes from viscous body fluids such as plasma or malignant ascites using differential centrifugation, it is necessary to include a dilution step to reduce the viscosity, and to increase both the centrifugal force and centrifugation time [41]. One possible drawback of using differential centrifugation for isolating exosomes is co-sedimentation of protein aggregates and co-purifying non-specifically bound proteins. As well as confounding the interpretation of MS-based protein identifications, it has been demonstrated that protein aggregates are ∼10,000 times more immunogenic than the corresponding soluble form because of preferential capture by antigen presenting cells [42]. One way of separating large protein aggregates from exosomes is by ultracentrifugation using a linear sucrose gradient to exploit their different flotation densities [43]; typically, exosomes have a

buoyant floatation density of 1.08–1.22 g/mL on sucrose gradients [37]. For the preparation of GMP-grade exosomes for clinical purposes, a combination of ultrafiltration, ultracentrifugation and a 30% sucrose/deuterium (D_2O) (98%) cushion (1.21 g/mL) has been recently described [44]. Interestingly, sucrose gradients have been shown to be inefficient in separating exosomes from HIV-1 particles due to similarities in their size/diameter and buoyant density. To overcome this problem, Cantin and colleagues describe the use of iodixanol (OptiPrep™) 6–18% gradients to separate HIV-1 particles and apoptotic vesicles from exosomes [45]. A rapid and simple method for isolating exosomes from culture media as well as body fluids is by immunoisolation employing magnetic beads. Exosome pull-down based on immunoaffinity can be a powerful isolation tool provided a specific exosomal cell surface protein can be identified that discriminates an exosome of interest from other membranous particles present in the biological matrix (for a list of exosomal protein markers see [43]). Immunoisolation of exosomes has been performed for antigen presenting cells [46], as well as HER2-positive exosomes from breast adenocarcinoma cell lines and ovarian cancer patient-derived ascites [47]. In addition, A33-positive exosomes released from colon carcinoma cancer cells [48], and EpCAM-positive exosomes from the sera of lung cancer [8] and ovarian cancer [28] patients have been obtained.

In this study, the culture medium of LIM1863 colorectal carcinoma cells was used to compare the morphological and proteomic profiles of exosomes purified by three different isolation strategies: ultracentrifugation (UC-Exos), density gradient centrifugation using OptiPrep™ (DG-Exos), and immunoisolation using EpCAM antibodies coupled to magnetic beads (IAC-Exos). To assess the three purification strategies we monitored the enrichment of several protein classes that have been inextricably associated with exosome biogenesis and/or function – endosomal sorting complex required for transport (ESCRT)-complex and their associated proteins, Rab GTPases, tetraspanins, proteins implicated in intracellular trafficking, as well as proteins that may be involved in exosome internalisation in a recipient cell. To enable this comparative enrichment assessment, we employed a proteomic label-free peptide spectral count strategy that entails summating the number of significant peptide MS/MS spectra for each individual protein, and normalising them with respect to the total number of spectra identified in that particular sample. The normalised ratios can then be compared between samples to estimate enrichment. Our findings indicate that immunoaffinity capture was the most efficient technique to enrich for exosomes compared to differential centrifugation and density gradient isolation methods.

2. Material and methods

2.1. Cell culture and preparation of concentrated culture medium (CCM)

Human colon carcinoma LIM1863 cells [49] were cultured in RPMI-1640 medium (Invitrogen, Carlsbad, CA) containing 5% FCS, α-thioglycerol (10 μM), insulin (25 units/L), hydrocortisone (1 mg/L), with 10% CO_2 at 37 °C. LIM1863 cells (∼2 × 10⁹ cells) were washed four times with 30 mL of RPMI-1640 media and cultured for 24 h in 750 mL serum-free RPMI-media supplemented with 0.6% insulin–transferrin–selenium (ITS) solution from Invitrogen. Approximately 750 mL of culture medium (CM) was collected and centrifuged at 4 °C (480g for 5 min followed by 2000g for 10 min) to remove intact cells and cell debris. CM was filtered using a VacuCap® 60 filter unit fitted with a 0.1 μm Supor® membrane (Pall Life Sciences, Port Washington, NY) and then concentrated to 1.5 mL using an Amicon® Ultra-15, Ultracel centrifugal filter device with a 5 K nominal molecular weight limit (NMWL)

(Millipore, MA, USA). The protein content of the concentrated culture medium (CCM) was estimated by 1D-SDS–PAGE/SYPRO® Ruby protein staining densitometry [50]. Briefly, a 5 μL aliquot was solubilised in SDS sample buffer (2% sodium dodecyl sulphate, 125 mM Tris–HCl, pH 6.8, 12.5% glycerol, 0.02% bromophenol blue) and loaded into 1 mm 10 well NuPAGE™ 4–12% (w/v) Bis–Tris Precast gel (Invitrogen). Electrophoresis was performed at 150 V for 1 h in NuPAGE™ 1× MES running buffer (Invitrogen) using an Xcell Surelock™ gel tank (Invitrogen). After electrophoresis, the gel was removed from the tank and fixed in 50 mL fixing solution (40% (v/v) methanol, 10% (v/v) acetic acid in water) for 30 min on an orbital shaker and then stained with 30 mL SYPRO® Ruby (Molecular Probes) for 30 min, followed by destaining twice in 50 mL of 10% (v/v) methanol with 6% (v/v) acetic acid in water for 1 h. The gel was imaged on a Typhoon 9410 variable mode imager (Molecular Dynamics), using a green (532 nm) excitation laser and a 610BP30 emission filter at 100 μm resolution. Densitometry quantitation was performed using ImageQuant software (Molecular Dynamics) to determine protein concentration relative to a BenchMark™ Protein Ladder standard of known protein concentration (Invitrogen).

2.2. Ultracentrifugation exosome (UC-Exo) isolation

Exosomes were isolated from CCM (500 μL, 1.5 mg protein) by centrifugation at 100,000g (TLA-45 fixed angle, Beckman Coulter) for 1 h at 4 °C. The pellet was resuspended in 1 mL PBS and re-centrifuged (100,000g, 1 h) (UC-Exos). UC-Exos (~375 μg protein) were resuspended in 50 μL PBS and either used immediately or stored at −80 °C.

2.3. OptiPrep™ density gradient exosome (DG-Exo) isolation

To prepare the discontinuous iodixanol gradient, 40% (w/v), 20% (w/v), 10% (w/v) and 5% (w/v) solutions of iodixanol were made by diluting a stock solution of OptiPrep™ (60% (w/v) aqueous iodixanol from Axis-Shield PoC, Norway) with 0.25 M sucrose/10 mM Tris, pH 7.5. The gradient was formed by adding 3 mL of 40% iodixanol solution to a 14 × 89 mm polyallomer tube (Beckman Coulter), followed by careful layering of 3 mL each of 20% and 10% solutions, and 2.5 mL of 5% solution. CCM (500 μL, 1.5 mg protein) was overlaid onto the top of the gradient, and centrifugation performed at 100,000g for 18 h at 4 °C. Twelve individual 1 mL gradient fractions were collected manually (with increasing density). Fractions were diluted with 2 mL PBS and centrifuged at 100,000g for 3 h at 4 °C followed by washing with 1 mL PBS, and resuspended in 50 μL PBS. Fractions were monitored for the expression of exosomal markers Alix, TSG101, and HSP70 by Western blotting. DG-Exos (yield ~150 μg) were stored at −80 °C until further use. To determine the density of each fraction, a control OptiPrep™ gradient containing 500 μL of 0.25 M sucrose/10 mM Tris, pH 7.5 was run in parallel. Fractions were collected as described, serially diluted 1:10,000 with water, and the iodixanol concentration determined by absorbance at 244 nm using a molar extinction coefficient of 320 L g^{-1}cm^{-1} [51].

2.4. EpCAM immunoaffinity capture exosome (IAC-Exo) isolation

Exosomes were isolated from LIM1863 cells using EpCAM (CD326) magnetic microbeads (Miltenyi Biotec, Auburn, CA), according to manufacturer's instructions. Briefly, 500 μL of CCM (1.5 mg protein) was incubated with EpCAM-microbeads (100 μL) for 4 h at 4 °C. An empty 3 mL LS Microcolumn was placed in a solid support magnet (SSM) and rinsed three times with Rinsing Solution (MACS® BSA Stock Solution diluted 1:20 with autoMACS® Rinsing Solution, Miltenyi Biotec). Exosome-bound microbeads were pipetted into the column and washed three times with

1 mL Rinsing Solution. The column was removed from the SSM and exosome-bound microbeads were recovered by rinsing the column at room temperature three times with 1 mL Rinsing Solution. Exosome-bound microbeads were washed twice with 1 mL PBS and centrifuged at 100,000g for 1 h at 4 °C. The supernatant was removed and IAC-Exos (yield ~195 μg) were eluted from the microbeads with either 100 μL of 0.2 M glycine, Tris–HCl, pH 2.8 for EM imaging, or lysed with 100 μL of SDS sample buffer for PAGE analysis.

2.5. Western blot analysis

Exosome samples (~10 μg protein) were lysed in SDS sample buffer with 50 mM DTT, heated for 5 min at 95 °C and subjected to electrophoresis using precast Novex 4–12% Bis–Tris NuPAGE gels (Invitrogen) in MES running buffer at constant 150 V for 1 h. Proteins were electrotransferred onto nitrocellulose membranes using the iBlot™ Dry Blotting System (Invitrogen), and the membranes blocked with 5% (w/v) skim milk powder in Tris-buffered saline with 0.05% (v/v) Tween-20 (TTBS) for 1 h at RT. Membranes were probed with primary mouse anti-TSG101 (BD Biosciences; 1:500), mouse anti-HSP70 (BD Biosciences; 1:1000), mouse anti-Alix (Cell Signaling Technology; 1:1000), for 1 h in TTBS (50 mM Tris, 150 mM NaCl, 0.05% Tween 20) followed by incubation with the secondary antibody, IRDye 800 goat anti-mouse IgG (1:15000, Li-COR Biosciences), for 1 h in darkness. All antibody incubations were carried out using gentle orbital shaking at room temperature. Western blots were washed three times in TTBS for 10 min after each incubation step and visualised using the Odyssey Infrared Imaging System, v3.0 (Li-COR Biosciences, Nebraska USA).

2.6. Electron microscopy (EM)

EM imaging of exosome preparations were performed as previously described [48], with slight modifications. Briefly, exosome preparations (~2 μg protein) were fixed in 1% (v/v) glutaraldehyde, layered onto formvar-coated 200 mesh copper grids (ProSciTech, Queensland, Australia), and allowed to dry at RT. Grids were then washed twice with water for 5 min, and stained with 1% (w/v) uranyl acetate in water (ProSciTech, Queensland, Australia) for 10 min. Imaging was performed at an acceleration voltage of 200 kV using a Gatan UltraScan 1000 (2 × 2 k) CCD (charge-coupled device) camera coupled to a Tecnai F30 (FEI, Netherlands) electron microscope.

2.7. GeLC–MS/MS

Exosome samples (20 μg) were separated by SDS–PAGE [52] and proteins visualised by Imperial Protein Stain (Pierce), according to the manufacturer's instructions. Gel lanes were cut into 20 × 2 mm bands using a GridCutter (The Gel Company, San Francisco, CA), and individual bands subjected to in-gel reduction, alkylation and trypsinisation as previously described [52]. Briefly, gel bands were reduced with 10 mM DTT (Calbiochem) for 30 min, alkylated for 20 min with 25 mM iodoacetic acid (Fluka), and digested with 150 ng trypsin (Worthington) for 4.5 h at 37 °C. Extracted tryptic peptides were concentrated to ~10 μL by centrifugal lyophilisation, and analysed by LC–MS/MS. RP-HPLC was performed on a nanoAcquity® (C18) 150 × 0.15 mm i.d. reversed phase UPLC column (Waters), using an Agilent 1200 HPLC, coupled online to an LTQ-Orbitrap mass spectrometer equipped with a nanoelectrospray ion source (Thermo Fisher Scientific) [53]. The column was developed with a linear 60 min gradient with a flow rate of 0.8 μL/min at 45 °C from 0% to 100% solvent B where solvent A was 0.1% (v/v) aqueous formic acid and solvent B was 0.1% (v/v) aqueous formic acid/60% acetonitrile. Survey MS scans

were acquired with the resolution set to a value of 30,000. Real time recalibration was performed using a background ion from ambient air in the C-trap [54]. Up to five of selected target ions were dynamically excluded from further analysis for 3 min.

2.8. Database searching and protein identification

Parameters used to generate peak lists, using Extract-MSn as part of Bioworks 3.3.1 (Thermo Fisher Scientific), were as follows: minimum mass 700; maximum mass 5000; grouping tolerance 0 Da; intermediate scans 200; minimum group count 1; 10 peaks minimum and TIC of 100. Peak lists for each LC–MS/MS run were merged into a single MGF file for Mascot searches. Automatic charge state recognition was used due to the high resolution survey scan (30,000). LC–MS/MS spectra were searched against the human RefSeq [55] protein database (38,791 sequences) using Mascot (v2.2.01, Matrix Science, UK). Searching parameters used were: fixed modification (carboxymethylation of cysteine; +58 Da), variable modifications (oxidation of methionine; +16 Da), three missed tryptic cleavages, 20 ppm peptide mass tolerance and 0.8 Da fragment ion mass tolerance. An MS/MS spectrum is deemed significant if its Mascot ion score is greater than its identity score. The ion score for an MS/MS spectrum is defined as $-10 \times \log 10(P)$, where P is the absolute probability that the observed match between the experimental data and the database sequence is a random event. The identity score is the significance threshold that indicates a 5% or lower probability that the MS/MS spectrum has been randomly matched to a sequence in the database [56]. Proteins were deemed to be significant if at least two unique peptides were identified. The false-discovery rate (derived from corresponding decoy database search [57]) was less than 0.3% for each exosome preparation.

Gene Ontology (GO) annotation was retrieved from the Human Protein Reference Database (HPRD) [58]. Protein sequence analysis of exosome proteins was performed to identify significantly enriched domains/motifs using SMART [59]. The transmembrane (TM) domain prediction tool TMHMM [60] was used to predict the presence of TM domains in the protein sequences that were identified by MS. Proteomic data from previous exosome studies was downloaded from ExoCarta [61,62] (http://www.exocarta.org), an exosome database containing all exosome proteins identified from multiple organisms.

2.9. Label-free spectral counting

The relative abundance of a protein within a sample was estimated using semi-quantitative normalised spectral count ratios (N_{sc}). For each individual protein, significant peptide MS/MS spectra were summated, and normalised by the total number of significant MS/MS spectra identified in the sample (Eq. (1))

$$N_{sc} = (n+f)/(t-n+f) \qquad (1)$$

where n is the number of significant peptide spectral counts for each protein in the sample, t is the total number of significant MS/MS spectral counts identified in the sample and f is the correction factor set to 1.25. A correction factor was used to allow an N_{sc} value to be calculated when $n = 0$.

To compare relative protein abundance between samples A and B, normalised spectral count ratios (R_{sc}) were determined using Eq. (2), a formula previously described in [63], based on work by [64,65]

$$R_{sc} = [(n_B+f)(t_A-n_A+f)]/[(n_A+f)(t_B-n_B+f)] \qquad (2)$$

where n is the significant protein spectral count, t is the total number of significant MS/MS spectra in the sample, f is a correction factor set to 1.25, and t_A and t_B are the samples being compared.

3. Results and discussion

Robust methods to purify exosomes from cell culture medium are dependent upon the ability to minimise co-purifying protein aggregates and other membranous particles. Differential centrifugation is limiting in this regard, and although it is the most commonly used technique to isolate exosomes, more specific/selective separation methods are required. Here we describe three strategies for purifying colon tumour-derived exosomes from the cell culture medium of LIM1863 cells [49]. Ultracentrifugation (UC-Exos), density gradient centrifugation using OptiPrep™ (DG-Exos), and immunoaffinity capture (IAC-Exos) using an antibody directed towards the epithelial cell adhesion molecule EpCAM (CD326) (see Fig. 1).

The efficacy of the three exosome purification strategies was monitored by EM, and the enrichment of typical exosomal markers such as Alix, TSG101, and HSP70 was assessed using Western blot analysis, as well as proteome profiling. As exosomes are of endosomal origin they typically contain proteins involved in multivesicular body (MVB) biogenesis, membrane transport and fusion (e.g., RabGTPases) [66], tetraspanins and their associated proteins that are functionally organised into tetraspanin-enriched microdomains – also referred to as the tetraspanin web [67], and proteins that may be involved in downstream exosome recognition and internalisation in a recipient cell [68]. Proteome profiling using mass spectrometry and label-free spectral counting [63] was employed to determine enrichment of these protein classes in the three purification methods studied.

3.1. Preparation of cell culture medium (CM) from LIM1863 cells

The colon cancer cell line LIM1863 was established in 1987 by Whitehead et al. [49], from a resected invasive human colon carcinoma, which had extended through the muscle wall of the colon. LIM1863 cells grow as free-floating suspension clusters, and contain differentiated columnar and goblet cells. These are the two main cell types found in colonic crypts which line the lumen
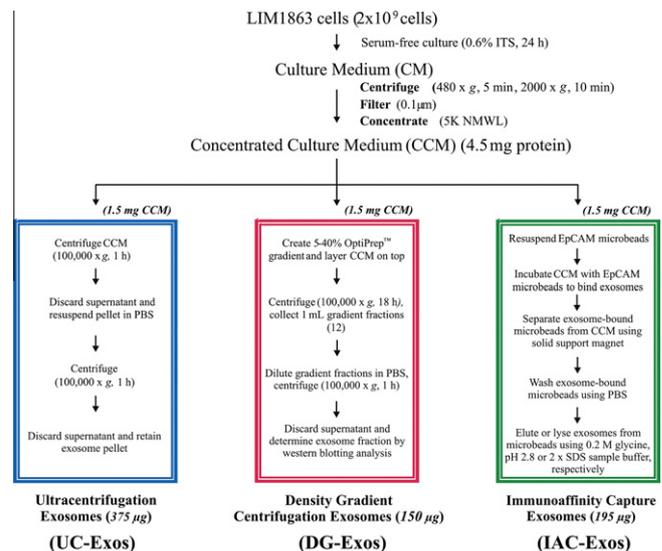
Fig. 1. Exosome isolation. Three experimental workflows were employed to isolate exosomes from human colon cancer LIM1863 cell culture medium (CM). Cells were grown in serum-free medium supplemented with insulin–transferrin–selenium (ITS) for 24 h, and CM collected, centrifuged, filtered, and concentrated (CCM) to yield approximately 4.5 mg protein. Exosomes were isolated from CCM (1.5 mg protein) by the following strategies: ultracentrifugation at 100,000g (UC-Exos), OptiPrep™ density gradient centrifugation (DG-Exos), or EpCAM immunoaffinity capture (IAC-Exos).

while undifferentiated cells localise at the periphery of the spheres [49,69]. Phase contrast microscopy shows that LIM1863 cells resemble an enclosed crypt *in vitro* (Supplementary Fig. S1A). To evaluate the polarity of the cells in the organoid, confocal microscopy was performed on LIM1863 cells stained with syntaxin 3 (apical marker) and A33 (basolateral marker) antibodies. Supplementary Fig. S1B shows polarised LIM1863 cells are arranged around a central lumen, with localisation of syntaxin 3 at the apical ring/organoid lumen (red), while A33 is primarily localised to the basolateral cell periphery (green).

LIM1863 cells were grown in serum-free media for 24 h to enable exosome collection in the presence of reduced FCS contaminants. Based on LDH and MTT assays, no significant differences in cell viability or cell proliferation were observed between FCS and serum-free culture containing 0.6% ITS (Supplementary Fig. S1C and D). The CM was depleted of intact cells and cell debris as well as large nanomembraneous particles (i.e., >100 nm) [18] by low-speed centrifugation, followed by filtration through a 100 nm membrane; the filtered CM was then concentrated to ~1.5 mL by centrifugal filtration using a 5 K NMWL membrane filter (Fig. 1).

3.2. Characterisation of exosomes isolated by ultracentrifugation (UC-Exos)

The first exosome isolation strategy examined was the commonly utilised ultracentrifugation procedure [43] consisting of centrifugation at 100,000g for 1 h (Fig. 1). The yield of UC-Exos was typically ~375 µg of protein from ~6×10^8 cells. Western blot analysis of UC-Exos revealed the presence of exosome markers Alix, HSP70, and TSG101 (Fig. 2A). Morphological analysis of the UC-Exos using EM revealed a heterogeneous population of vesicles comprising both round-shaped 40–100 nm diameter vesicles, consistent with exosomes [1], as well as larger vesicles slightly clumped together (Fig. 2A). While the nature of the larger vesicles is unknown, presumably it is not due to multiple ultracentrifugation steps and/ or deep-freezing and thawing since these handling steps have been reported not to affect exosome size [70].

We next examined the proteome profile of the UC-Exos using GeLC–MS/MS [52] and identified 728 unique proteins (Supplementary Table S1 and Fig. S2). The most abundant proteins, based upon the number of spectra identified, contain subunits of high M_r complexes, such as major vault protein (MVP) [71], the 26S proteasome complex [72], heparan sulphate proteoglycan 2 (HSPG2), and fatty acid synthase (FASN), which comprises two M_r ~270 K multifunctional polypeptide chains, each containing seven discrete functional domains [73]. Given that these proteins have been shown to sediment at high centrifugal force, they may represent artefacts of the UC-Exo purification strategy.

To ascertain the relative abundance of a particular protein within a sample, label-free spectral counting was performed. For each protein within an exosome sample, the total number of significant tryptic peptide spectra identified for that particular protein was summed and normalised by the total number of significant peptide spectral counts in the sample (see Eq. (1)). Thus, a higher normalised spectral count ratio (N_{sc}) reflects higher protein abundance. N_{sc} values for the following exosome-associated protein classes are graphically represented in Fig. 3: ESCRT complex components, Rab GTPases, tetraspanins, and proteins involved in trafficking, release, recognition, and uptake. Albeit at low levels, several of these exosome-associated proteins were identified in UC-Exos. Conspicuous amongst these was the relatively high expression levels of Alix (Fig. 3A). Alix is not only linked to ESCRT-mediated endosomal protein sorting, but is also involved in regulating other cellular mechanisms including growth factor receptor endocytosis, enveloped budding from the PM, and remodelling of focal adhesions (for a review see [74]) – which might explain the high expression levels seen in UC-Exos.

3.3. Characterisation of exosomes purified by density gradient centrifugation (DG-Exos)

In an effort to minimise protein contamination from large protein aggregates that co-sediment with exosomes during ultracentrifugation, we next evaluated the ability to exploit the buoyant
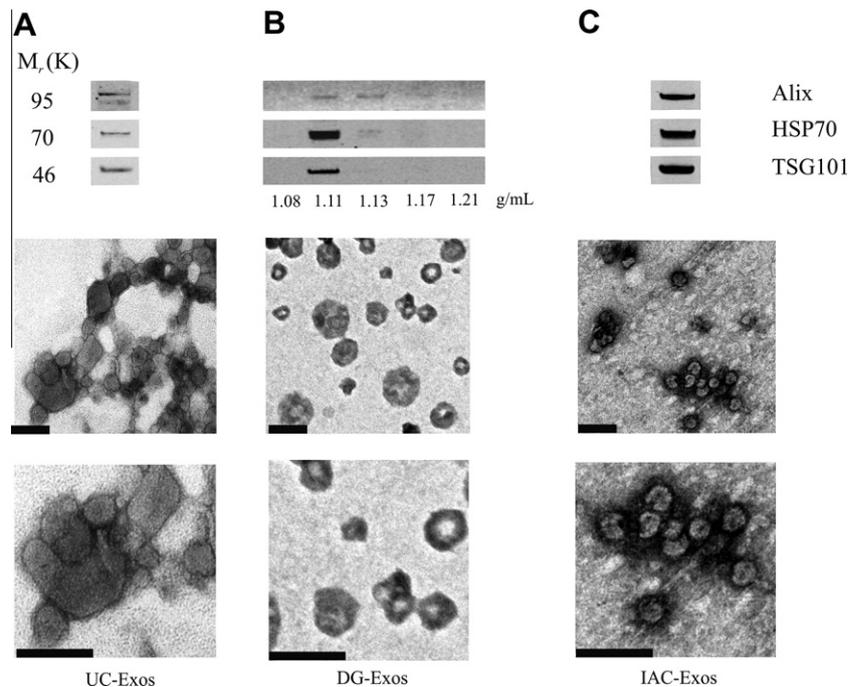
Fig. 2. Characterisation of exosomes. UC-Exos (A), DG-Exos (B), and IAC-Exos (C) were characterised by Western blotting and electron microscopy. For Western blotting, each exosome preparation (10 µg) was separated by 1D-SDS–PAGE, electrotransferred, and probed with exosome markers Alix, HSP70, and TSG101. Exosomes from each purification strategy were negatively stained using uranyl acetate and viewed by electron microscopy. The scale bar represents 100 nm.

density of exosomes for purification. Although sucrose density gradient centrifugation, either continuous [37] or discontinuous gradients (i.e., sucrose cushion [44]), has been used extensively to purify exosomes it is well known that these methods do not allow separation of exosomes from viruses or large microvesicles with comparable sedimentation velocities [45]. One way of overcoming this limitation involves substituting sucrose with iodoxanol (OptiPrep™) in the velocity gradient [45]. Fig. 1 outlines the strategy for purifying LIM1863-derived exosomes using a 5–40% OptiPrep™ density gradient (DG-Exos). Western blot analysis of 1 mL fractions following OptiPrep™ density gradient separation indicated that LIM1863 cell-derived exosomes were enriched at a buoyant density of 1.11 g/mL, based on the expression of exosome markers Alix, TSG101, and HSP70 (Fig. 2B). This density is
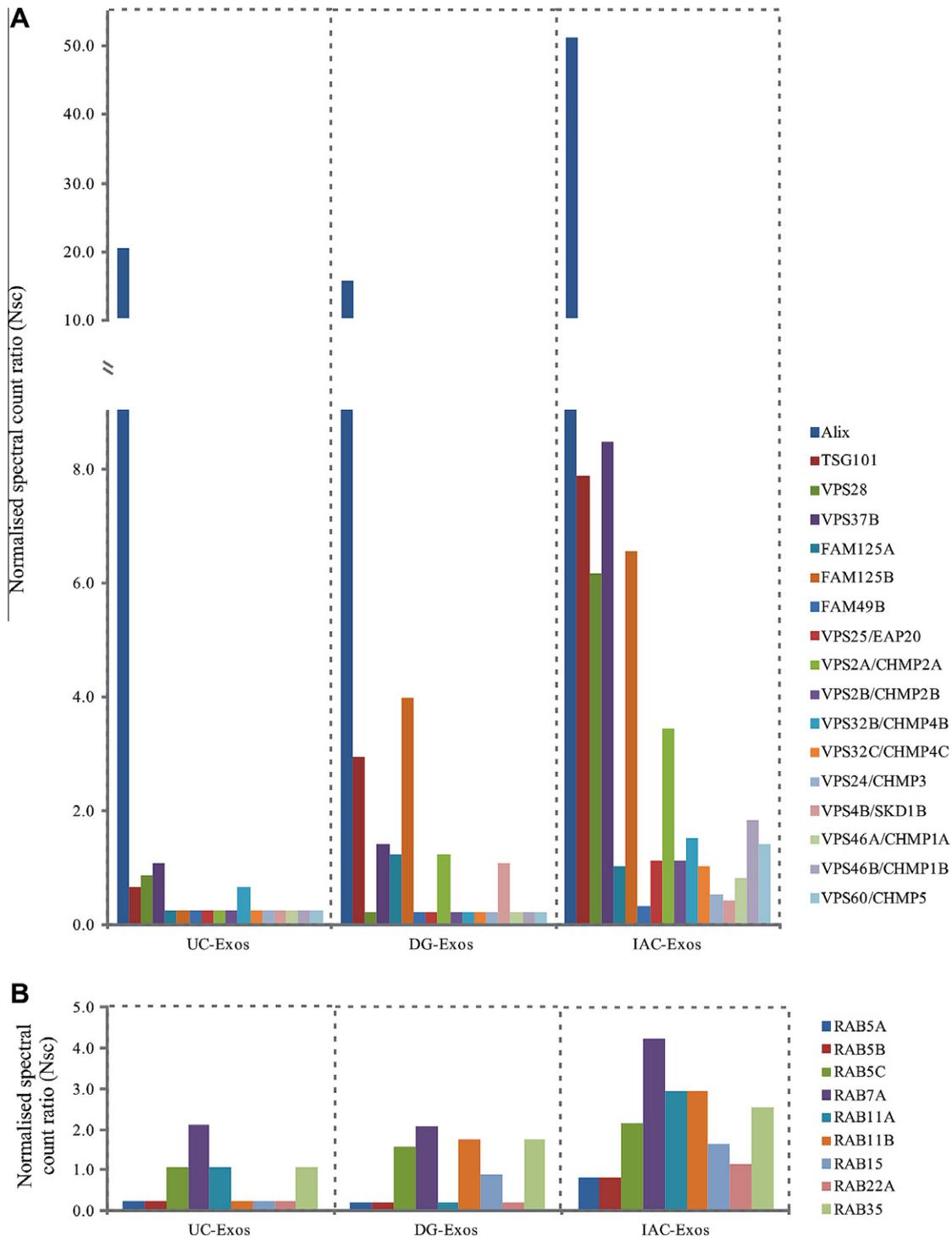
Fig. 3. Semi-quantitative normalised spectral count ratios of selected exosome proteins. The relative abundance of a proteins (containing at least two significant peptides) within a sample was estimated using semi-quantitative normalised spectral count ratios (N_{sc}). For each individual protein, significant peptide MS/MS spectra were summated, and normalised by the total number of significant peptide MS/MS spectra identified in the sample. The ratio serves an indicator of protein abundance, i.e., the higher the ratio, the more abundant the protein within the sample. Protein categories of interest included proteins associated with ESCRT components (A), Rab GTPases (B), tetraspanins (C), and trafficking, recognition, and exosome internalisation (D).
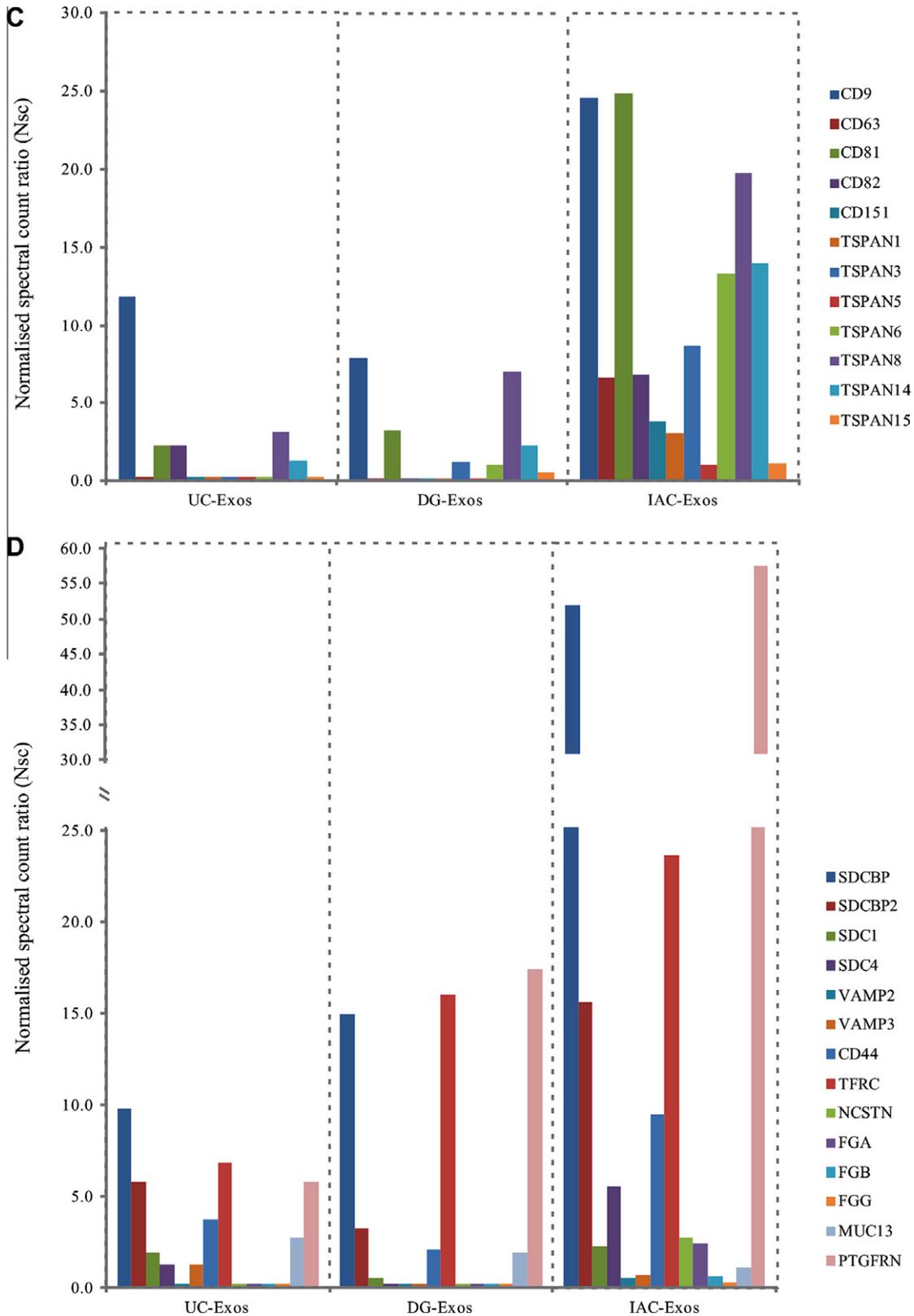
Fig. 3 (*continued*)

consistent with that reported for exosomes isolated from a diverse range of cell types including B lymphocytes [37]. The presence of Alix, and to a lesser extent HSP70, in the 1.13 g/mL density fraction suggests the presence of microvesicles other than exosomes in this preparation. The yield of exosomes in the 1.11 g/mL fraction (DG-Exos) was typically 150 μg/~6 × 10^8 LIM1863 cells. EM analysis of DG-Exos revealed a homogeneous population of vesicles that were round in shape, and had a size distribution in the range 50–100 nm, which is consistent with published reports for exosome morphology [1].

Proteomic profiling of LIM1863-derived DG-Exos identified 571 proteins (Supplementary Fig. S2), and revealed a diminution of many of the subunits of high-M_r proteins observed in the UC-Exos, including MVP, and fatty acid synthase (Supplementary Table S1). This finding suggests that these proteins are most likely artefacts in the UC-Exo preparation. Compared to UC-Exos, DG-Exos show increased abundance of ESCRT complex components (Fig. 3A, TSG101, and FAM125B), RabGTPases (Fig. 3B, Rab11B), tetraspanin 8 (Fig. 3C), and proteins TFRC (transferring receptor C) and PTGFRN (prostaglandin F2 receptor negative regulator) that may mediate uptake in recipient cells (Fig. 3D). Towards defining the relative abundance of a particular protein between samples, relative spectral count ratios were determined using the formula outlined in Eq. (2). For example, the expression of the ESCRT accessory protein KIAA0174 was estimated to be increased by 19.4-fold in DG-Exos compared to UC-Exos (Table 1). Another notable difference between the UC- and DG-Exos was the marked enrichment of plasma membrane proteins based on GO-annotation (HPRD:GO:0005886) and TMHMM predicted transmembrane domains [60]. For example, 120/728 (16%) proteins in UC-Exos were PM proteins, compared with 154/571 (27%) in DG-Exos (Supplementary Fig. S3).

3.4. Characterisation of exosomes purified by EpCAM immunoaffinitycapture (IAC-Exos)

Due to the incomplete separation of exosomes into the 1.1 g/mL density fraction (Fig. 2B), we decided to evaluate a biospecific method. Immunoaffinity capture relies upon magnetic beads coated with monoclonal antibodies directed against a specific exosomal membrane surface protein (Fig. 1). Immunoaffinity capture has been previously employed to isolate exosomes from colon tumour cells (A33 mAb [48]), Jurkat T cells (CD45 mAb [75]), breast adenocarcinoma cells (HER2 mAbs [47], and EpCAM mAbs for lung [8] and ovarian circulating exosomes [28]. In this study, we utilised magnetic beads coated with antibodies targeting the epithelial cell adhesion molecule EpCAM (CD326), which is found to be over expressed on epithelial progenitors, carcinomas, and cancer-initiating cells [76]. For a review see [77].

Purification of IAC-Exos typically yielded 195 μg protein from $\sim 6 \times 10^8$ LIM1863 cells. EM analysis of IAC-Exos also revealed a homogeneous population of vesicles round in shape and with a size distribution in the range 40–60 nm, however these vesicles had a more homogenous morphology (Fig. 2C). Overall, 627 IAC-Exo proteins were unambiguously identified (Supplementary Table S1 and Fig. S2). In contrast to UC- and DG-Exo preparations, IAC-Exos are dominated by proteins involved in MVB biogenesis, RabGTPases, and proteins involved in protein trafficking. For example, the vacuolar protein sorting 28 homolog had 7- and 28.8-fold increased expression in IAC-Exos, compared to UC-Exos and DG-Exos, respectively (Table 1).

According to semi-quantitative spectral counting, the most abundant proteins identified in IAC-Exos were Eph receptors B2 and B3 (EPHB2, EPHB3), which are reported to be involved in tumour cell migration and angiogenesis [78], integrin alpha 6 (ITGA6), as well as Alix. IAC-Exos were also enriched in PM proteins compared to UC-Exos and DG-Exos, as 201/627 (32%) had PM annotation based on GO annotation (Supplementary Fig. S3).

3.5. Exosome markers most significantly enriched in IAC-Exos

Based on N_{sc} values in Fig. 3, and R_{sc} ratios for exosome markers in Table 1, it is clearly evident that the immunoaffinity isolation technique was the superior strategy for enriching for colon cancer cell-derived exosomes. Further, detailed interrogation of the IAC-Exo dataset of 627 proteins revealed a protein signature reflecting exosome biogenesis, trafficking, and proteins that may potentially mediate an interaction or uptake in a recipient cell.

The sorting of cytoplasmic cargo proteins into ILVs (exosomes) involves several mechanisms including the ESCRT machinery, lipids, and/or tetraspanin-enriched microdomains [79]. The ESCRT machinery comprises four complexes (0, I–III) and several accessory components, which control invagination of the MVB limiting membrane and formation of ILVs [80]. Several components of the ESCRT complex machinery were identified in IAC-Exos (Fig. 3A and Table 1). These include components of ESCRT-I (TSG101, VPS28, VPS37B, and FAM proteins 49B, 125A, and 125B), ESCRT-II (VPS25/EAP20), ESCRT-III (VPS2A/CHMP2A, VPS2B/CHMP2B, VPS24/CHMP3, VPS32B/CHMP4B, and VPS32C/VHMP4C), and the ESCRT accessory components of VPS4 (VPS4B/SKD1B, VPS46A/CHMP1A, VPS46B/CHMP1B, and VPS60/CHMP5).

It can be seen in Fig. 3B and C that IAC-Exos are significantly enriched with members of the family of RabGTPases and proteins that may be involved in assisting exosome recognition and internalisation in a recipient cell. While all exosomes reported thus far, regardless of cell type from which they originate, have been reported to contain RabGTPases, $M_r \sim 20$ K proteins associated with the docking and fusion of secretory vesicles to the plasma membrane (i.e., exocytosis) [81], it is not clear whether this family of molecules resides within exosomes, or are associated with trace amounts of immature vesicles that emerge from Golgi and/or endosomes. Prominent RabGTPases enriched in IAC-Exos include the endosome-resident RabGTPase isoform 11b, which is thought to control crosstalk between the endocytic and secretory pathways [82,83], and Rab35 that regulates exosome secretion by assisting docking and tethering of MVB's to the plasma membrane [84].

Other Rabs identified in IAC-Exos include Rabs 5a, 5b, 5c, 7a, 11a, 15, and 22a, as well as ADP-ribosylation factor (ARF6). Previous studies have reported the involvement of Rabs 5, 11, 27a, and 27b in exosome release [83,85]. More specifically, Rab5 mediates endocytosis from the plasma membrane, while Rab7 is involved in trafficking away from the late endosome [86]. ARF6 is involved in receptor-mediated endocytosis [87] and exocytosis of intracellular vesicles from the recycling endosomes to the plasma membrane [88,89]. Similarly, syntenin (SDCBP, SDCBP2) and syndecan proteins (SDC1, SDC4) have been linked to trafficking and recycling from endosomes to the plasma membrane [90]. In addition to Rab and ARF GTPases, soluble NSF attachment protein receptor (SNARE) molecules are key components of molecular machinery involved in the recognition and fusion of membranes [91]. In this study, vesicle-associated membrane proteins VAMP2 and VAMP3 were identified. Belonging to the SNARE family, VAMPs (or synaptobrevins) are anchored in the vesicular membrane and mediate intracellular vesicle fusion [68,92]. These proteins have also been reported previously across multiple exosome studies [61].

Conspicuously, several GPI-anchor proteins (CD59, CEACAM5, MFI2, NT5E, and XPNPEP2) were identified in IAC-Exos (Table 1). It has also been suggested that proteins with affinity for "raft-like domains" such as tetraspanins are involved in the sorting of cargo into ILVs [79]. Since tetraspanins are known to form protein complexes and function in highly ordered raft-like domains [93], it seems likely that they may be involved in exosome biogenesis. The tetraspanins CD9, CD63, CD81, CD82, CD151, TSPAN1, TSPAN3, TSPAN5, TSPAN6, TSPAN8, TSPAN14, and TSPAN15 were significantly enriched in IAC-Exos compared to UC-Exos and DG-Exos (Fig. 3C and Table 1). Interestingly, tetraspanin TSPAN8 has been recently found to mediate selective recruitment of proteins and mRNA into exosomes in rat adenocarcinoma cells [94].

The molecular mechanisms governing exosome recognition and internalisation remain largely unknown [95]. However, current hypotheses include exosomes either binding to the cell surface, or direct fusion with the plasma membrane, or internalisation

Table 1
Relative quantification of selected exosome proteins by label-free spectral counting.

	Category	Gene ID	Gene symbol	Protein name	R_{SC} (DG/UC)[a]	R_{SC} (IAC/UC)[b]	R_{SC} (IAC/DG)[c]	ExoCarta[d]
Exosome biogenesis	ESCRT-I	7251	TSG101	Tumour susceptibility gene 101	4.4	11.7	2.7	Y
		51160	VPS28	Vacuolar protein sorting 28 homolog	−4.1	7.0	28.8	Y
		79720	VPS37B	Vacuolar protein sorting 37 homolog B	1.3	7.8	6.0	Y
		93343	FAM125A	Family with sequence similarity 125, member A	4.8	4.0	−1.2	Y
		89853	FAM125B	Family with sequence similarity 125, member B	15.4	25.5	1.6	Y
		51571	FAM49B	Family with sequence similarity 49, member B	−1.2	1.3	1.5	Y
	ESCRT-II	84313	VPS25/EAP20	Vacuolar protein sorting 25 homolog	−1.2	4.4	5.3	Y
	ESCRT-III	27243	VPS2A/CHMP2A	Chromatin modifying protein 2A	4.8	13.3	2.8	Y
		25978	VPS2B/CHMP2B	Chromatin modifying protein 2B	−1.2	4.4	5.3	Y
		128866	VPS32B/CHMP4B	Chromatin modifying protein 4B	−3.1	2.3	7.2	Y
		92421	VPS32C/CHMP4C	Chromatin modifying protein 4C	−1.2	4.0	4.8	
		51652	VPS24/CHMP3	Vacuolar protein sorting 24 homolog	−1.2	2.0	2.5	Y
	ESCRT Accessory	10015	ALIX/PDCD6IP	Programmed cell death 6 interacting protein	−1.3	2.5	3.3	Y
		9525	VPS4B/SKD1B	Vacuolar protein sorting four homolog B	4.1	1.7	−2.5	Y
		5119	VPS46A/CHMP1A	Chromatin modifying protein 1A	−1.2	3.2	3.9	Y
		57132	VPS46B/CHMP1B	Chromatin modifying protein 1B	−1.2	7.1	8.6	Y
		51510	VPS60/CHMP5	Chromatin modifying protein 5	−1.2	5.6	6.7	Y
		9798	KIAA0174	KIAA0174	19.4	24.3	1.3	Y
	GPI-anchor	966	CD59	CD59 molecule, complement regulatory protein	−1.2	6.7	8.1	Y
		1048	CEACAM5	Carcinoembryonic antigen-related cell adhesion molecule 5	−17.6	−1.8	10.0	Y
		4241	MFI2	Antigen p97	−1.2	2.8	3.4	Y
		4907	NT5E	5′-nucleotidase, ecto (CD73)	4.8	13.0	2.7	Y
		7512	XPNPEP2	X-prolyl aminopeptidase (aminopeptidase P) 2	1.6	2.2	1.4	Y
	Tetraspanin	928	CD9	CD9 molecule	−1.5	2.1	3.1	Y
		967	CD63	CD63 molecule	−1.2	25.8	31.2	Y
		975	CD81	CD81 molecule	1.4	10.7	7.6	Y
		3732	CD82	CD82 molecule	−10.9	3.0	32.1	Y
		977	CD151	CD151 molecule	−1.2	14.9	18.0	Y
		10103	TSPAN1	Tetraspanin 1	−1.2	11.8	14.2	Y
		81619	TSPAN14	Tetraspanin 14	1.8	10.8	6.1	Y
		23555	TSPAN15	Tetraspanin 15	2.2	4.4	2.0	Y
		10099	TSPAN3	Tetraspanin 3	4.8	33.7	7.0	Y
		10098	TSPAN5	Tetraspanin 5	−1.2	4.0	4.8	Y
		7105	TSPAN6	Tetraspanin 6	4.1	51.7	12.5	Y
		7103	TSPAN8	Tetraspanin 8	2.2	6.3	2.8	Y
Trafficking and release	GTPase	5878	RAB5C	RAB5C	1.5	2.0	1.3	Y
		5868	RAB5A	RAB5A	−1.2	3.2	3.9	Y
		5869	RAB5B	RAB5B	−1.2	3.2	3.9	Y
		7879	RAB7A	RAB7A	−1.0	2.0	2.0	Y
		8766	RAB11A	RAB11A	−5.1	2.7	13.8	Y
		9230	RAB11B	RAB11B	6.8	11.4	1.7	Y
		376267	RAB15	RAB15	3.5	6.3	1.8	Y
		57403	RAB22A	RAB22A	−1.2	4.4	5.3	Y
		11021	RAB35	RAB35	1.6	2.3	1.4	Y
		382	ARF6	ADP-ribosylation factor 6	−4.1	5.2	21.3	Y
	Syntenin	27111	SDCBP2	Syndecan binding protein (syntenin) 2	−1.8	2.7	4.8	Y
		6386	SDCBP	Syndecan binding protein (syntenin)	1.5	5.3	3.5	Y
	Syndecan	6382	SDC1	Syndecan 1	−3.4	1.2	4.0	Y
		6385	SDC4	Syndecan 4	−6.0	4.3	26.0	Y
	SNARE	6844	VAMP2	Vesicle-associated membrane protein 2 (synaptobrevin 2)	−1.2	2.0	2.5	
		9341	VAMP3	Vesicle-associated membrane protein 3 (cellubrevin)	−6.0	−1.8	3.4	Y
Recognition and uptake	Internalisation motif	960	CD44	CD44 molecule (Indian blood group)	−1.8	2.5	4.5	Y
		7037	TFRC	Transferrin receptor (p90, CD71)	2.3	3.4	1.5	Y
	Protein binding domain	23385	NCSTN	Nicastrin	−1.2	10.6	12.8	Y
		2243	FGA	Fibrinogen alpha chain	−1.2	9.4	11.4	Y
		2244	FGB	Fibrinogen beta chain	−1.2	2.4	2.9	Y
		2266	FGG	Fibrinogen gamma chain	−1.2	1.3	1.5	Y
		56667	MUC13	Mucin 13, cell surface associated	−1.4	−2.4	−1.7	Y
		5738	PTGFRN	Prostaglandin F2 receptor negative regulator	3.0	9.9	3.3	Y
	MHC component	649853	HLA-A29.1	Major histocompatibility complex class I HLA-A29.1	2.2	4.2	1.9	Y
		3105	HLA-A	Major histocompatibility complex, class I, A	3.7	6.0	1.6	Y
		3107	HLA-C	Major histocompatibility complex, class I, C	1.6	2.1	1.3	Y

[a] Relative spectral count ratio (R_{sc}) for proteins identified in DG-Exos, compared with UC-Exos (Eq. (2)).
[b] Relative spectral count ratio (R_{sc}) for proteins identified in IAC-Exos, compared with UC-Exos (Eq. (2)).
[c] Relative spectral count ratio (R_{sc}) for proteins identified in IAC-Exos, compared with DG-Exos (Eq. (2)).
[d] Presence of proteins in the exosome database ExoCarta [61,62].

[17]. Receptors which mediate exosome internalisation such as phosphatidylserine receptor Tim4 [96], LFA-1 [97], ICAM-1 [98], and intersectin-2 [99], a multimodular complex involved in clathrin-coated pit internalisation, were identified in IAC-Exos. In addition, various proteins containing 'short-sequence motif' required for internalisation were identified, including CD44, mannose-6-phosphate receptor, and transferrin receptor [100]. Further, whilst it remains speculative, we report several proteins of interest which may be involved in exosome recognition and uptake based on their protein binding GO Slim annotation. For example, nicastrin (NCSTN), fibrinogen (FGA, FGB, FGG), cell surface associated mucin 13 (MUC13), prostaglandin F2 receptor (PTGFRN), SDCBP2, and VAMP3 were present in the immunoaffinity dataset, and are also associated with cell communication and signal transduction (NCSTN, PTGFRN, SDCBP2). NCSTN, is an essential glycoprotein component of the γ-secretase complex, and is involved in regulating presenilin function and, importantly, intramembrane proteolysis of substrates associated with the transmembrane [101]. Expression of MUC1 on exosomes has been associated with inducing an immune response [102] and various MHC class I molecules were also identified in this study, including HLA-A, HLA-A29.1, and HLA-C.

3.6. Cancer related proteins in IAC-Exos

Of the 171 unique proteins identified in IAC-Exos (Supplementary Fig. S2), many are associated with cancer. Several proteins involved in cell proliferation and cancer cell invasion were identified in IAC-Exos (Supplementary Table S2). For example, proto-oncogene c-Met protein (hepatocyte growth factor receptor) is involved in tyrosine–protein kinase activity at the cell membrane. Dysregulated expression of c-Met has multifunctional effects in oncogenesis, and is implicated in cancer progression. Previously, c-Met-containing exosomes in rat pancreatic adenocarcinoma were shown to promote proliferation and induce gene expression in metastatic organ cells [103]. Similarly, amphiregulin (AREG) has been associated with tumour progression, including tissue invasion and metastasis of different human epithelial carcinoma types [104]. Higginbotham et al. have proposed that exosomes act as signalling platforms [23]. For example, they postulate that AREG is concentrated in exosomes in a manner that allows aggregation and oligomerisation of EGFR during receptor-ligand engagement, a new mode of exosomal targeted receptor activation (ExTRAcrine) [23]. Other cancer-related proteins that were identified in IAC-Exos include various ephrins (EFNB1, EFNB2) and Eph receptors (EPHA2–8, EPHB1–4), and components involved in Wnt (CTNNB1, TNIK) and Ras (CRK, GRB2) signalling (Supplementary Table S2). Ephrin/Eph signalling has been implicated in tumour progression via its ability to promote tumour cell motility and invasion [105]. More widely documented is the overexpression of both A- and B-type Eph receptors and their ephrin ligands, in specific tumours, including colon [106]. Further, we report the identification of the kinase TNIK, an important activator of Wnt target genes (i.e., TCF–LEF) in colon cancer [107]. In addition, we also identified CTNNB1 in both DG-Exos and IAC-Exos. β-Catenin, encoded by CTNNB1, is a nascent transcription factor that transmits signals from Wnt ligands to the nucleus [108]. Further studies will be required to investigate the role of exosomes as potential cargo mediators of Wnt signalling. Several key components associated with colorectal cancer were further identified in this study, including CEACAM1 and 5, FAT1, and CDH17. CEACAM5 (CEA) has been shown to be overexpressed in over 90% of human gastrointestinal and pancreatic cancers [109], and is associated with metastatic potential in colon cancer [110].

Apart from an enrichment of proteins associated with cancer, a salient finding in IAC-Exos was the identification of several proteins associated with the large 60S (22 proteins) and small 40S (eight proteins) subunits of the ribosomal complex. The biological significance remains to be confirmed, however, it is tempting to hypothesise that they impart some inter-cellular function in a recipient cell. A further finding of this study was the identification of membrane opsonisation complements CD46 (also identified in DG-Exos) and CD59 in IAC-Exos. It has been reported that expression of GPI-anchored complement regulators such as CD59 enhance survival in the extracellular environment [111].

4. Conclusion

While exosomes possess extensive diagnostic and therapeutic potential, a current obstruction hampering exosome research is the ability to obtain pure material. Towards rigorous biochemical and biophysical analysis, we have compared and evaluated three currently used isolation strategies including centrifugation, density-based separation, and EpCAM immunoaffinity capture to purify exosomes from LIM1863 cells. All preparations contained vesicles with sizes of 40–100 nm, and expression of exosome markers Alix, TSG101, and HSP70. However, immunoaffinity capture was evaluated to be the best method to capture exosomes, as it was able to enrich exosome markers, and exosome-associated proteins by at least twofold more than the other two methods studied. Protein, lipid, mRNA and miRNA analyses of highly purified vesicles will lead to significant advances in exosome characterisation, and facilitate a deeper understanding of their biological functions.

Conflict of interest

The authors declare no conflict of interest.

Appendix A. Supplementary data

Supplementary data associated with this article can be found, in the online version, at doi:10.1016/j.ymeth.2012.01.002.

References

[1] R.J. Simpson, J.W. Lim, R.L. Moritz, S. Mathivanan, Expert. Rev. Proteomics 6 (2009) 267–283.
[2] A. Bobrie, M. Colombo, G. Raposo, C. Thery, Traffic 12 (2011) 1659–1668.
[3] K. Skriner, K. Adolph, P.R. Jungblut, G.R. Burmester, Arthritis Rheum. 54 (2006) 3809–3814.
[4] M. Gonzalez-Begne, B. Lu, X. Han, F.K. Hagen, A.R. Hand, J.E. Melvin, J.R. Yates, J. Proteome Res. 8 (2009) 1304–1314.
[5] P.A. Gonzales, T. Pisitkun, J.D. Hoffert, D. Tchapyjnikov, R.A. Star, R. Kleta, N.S. Wang, M.A. Knepper, J. Am. Soc. Nephrol. 20 (2009) 363–379.
[6] A. Poliakov, M. Spilman, T. Dokland, C.L. Amling, J.A. Mobley, Prostate 69 (2009) 159–167.
[7] C. Admyre, S.M. Johansson, K.R. Qazi, J.J. Filen, R. Lahesmaa, M. Norman, E.P. Neve, A. Scheynius, S. Gabrielsson, J. Immunol. 179 (2007) 1969–1978.
[8] G. Rabinowits, C. Gercel-Taylor, J.M. Day, D.D. Taylor, G.H. Kloecker, Clin. Lung Cancer 10 (2009) 42–46.

[9] B.T. Pan, R.M. Johnstone, Cell 33 (1983) 967–978.
[10] R.M. Johnstone, M. Adam, J.R. Hammond, L. Orr, C. Turbide, J. Biol. Chem. 262 (1987) 9412–9420.
[11] R.M. Johnstone, Blood Cells Mol. Dis. 36 (2006) 315–321.
[12] N. Chaput, C. Thery, Semin. Immunopathol. 33 (2011) 419–440.
[13] C. Thery, M. Ostrowski, E. Segura, Nat. Rev. Immunol. 9 (2009) 581–593.
[14] T.L. Whiteside, Br. J. Cancer 92 (2005) 209–211.
[15] M. Iero, R. Valenti, V. Huber, P. Filipazzi, G. Parmiani, S. Fais, L. Rivoltini, Cell Death Differ. 15 (2008) 80–88.
[16] S. Keller, M.P. Sanderson, A. Stoeck, P. Altevogt, Immunol. Lett. 107 (2006) 102–108.
[17] M. Simons, G. Raposo, Curr. Opin. Cell Biol. 21 (2009) 575–581.
[18] S. Mathivanan, H. Ji, R.J. Simpson, J. Proteomics 73 (2010) 1907–1920.
[19] M.P. Sanderson, S. Keller, A. Alonso, S. Riedle, P.J. Dempsey, P. Altevogt, J. Cell. Biochem. 103 (2008) 1783–1797.
[20] F.I. Hawari, F.N. Rouhani, X. Cui, Z.X. Yu, C. Buckley, M. Kaler, S.J. Levine, Proc. Natl. Acad. Sci. USA 101 (2004) 1297–1302.
[21] K. Al-Nedawi, B. Meehan, J. Micallef, V. Lhotak, L. May, A. Guha, J. Rak, Nat. Cell Biol. 10 (2008) 619–624.
[22] S. Keller, A.K. Konig, F. Marme, S. Runz, S. Wolterink, D. Koensgen, A. Mustea, J. Sehouli, P. Altevogt, Cancer Lett. 278 (2009) 73–81.
[23] J.N. Higginbotham, M. Demory Beckler, J.D. Gephart, J.L. Franklin, G. Bogatcheva, G.J. Kremers, D.W. Piston, G.D. Ayers, R.E. McConnell, M.J. Tyska, R.J. Coffey, Curr. Biol. 21 (2011) 779–786.
[24] J.L. Hood, R.S. San, S.A. Wickline, Cancer Res. 71 (2011) 3792–3801.
[25] J. Skog, T. Wurdinger, S. van Rijn, D.H. Meijer, L. Gainche, M. Sena-Esteves, W.T. Curry Jr., B.S. Carter, A.M. Krichevsky, X.O. Breakefield, Nat. Cell Biol. 10 (2008) 1470–1476.
[26] H. Valadi, K. Ekstrom, A. Bossios, M. Sjostrand, J.J. Lee, J.O. Lotvall, Nat. Cell Biol. 9 (2007) 654–659.
[27] C. Subra, D. Grand, K. Laulagnier, A. Stella, G. Lambeau, M. Paillasse, P. De Medina, B. Monsarrat, B. Perret, S. Silvente-Poirot, M. Poirot, M. Record, J. Lipid Res. 51 (2010) 2105–2120.
[28] D.D. Taylor, C. Gercel-Taylor, Gynecol. Oncol. 110 (2008) 13–21.
[29] A. Delcayre, J.B. Le Pecq, Curr. Opin. Mol. Ther. 8 (2006) 31–38.
[30] J.S. Schorey, S. Bhatnagar, Traffic 9 (2008) 871–881.
[31] A. Tan, H. De La Pena, A.M. Seifalian, Int. J. Nanomed. 5 (2010) 889–900.
[32] L. Alvarez-Erviti, Y. Seow, H. Yin, C. Betts, S. Lakhal, M.J. Wood, Nat. Biotechnol. 29 (2011) 341–345.
[33] Y. Seow, M.J. Wood, Mol. Ther. 17 (2009) 767–777.
[34] J.G. van den Boorn, M. Schlee, C. Coch, G. Hartmann, Nat. Biotechnol. 29 (2011) 325–326.
[35] R.C. Lai, F. Arslan, M.M. Lee, N.S. Sze, A. Choo, T.S. Chen, M. Salto-Tellez, L. Timmers, C.N. Lee, R.M. El Oakley, G. Pasterkamp, D.P. de Kleijn, S.K. Lim, Stem Cell Res. 4 (2010) 214–222.
[36] P.E. Mangeot, S. Dollet, M. Girard, C. Ciancia, S. Joly, M. Peschanski, V. Lotteau, Mol. Ther. 19 (2011) 1656–1666.
[37] G. Raposo, H.W. Nijman, W. Stoorvogel, R. Liejendekker, C.V. Harding, C.J. Melief, H.J. Geuze, J. Exp. Med. 183 (1996) 1161–1172.
[38] H. Ji, N. Erfani, B.J. Tauro, E.A. Kapp, H.J. Zhu, R.L. Moritz, J.W. Lim, R.J. Simpson, Electrophoresis 29 (2008) 2660–2671.
[39] C. Thery, M. Boussac, P. Veron, P. Ricciardi-Castagnoli, G. Raposo, J. Garin, S. Amigorena, J. Immunol. 166 (2001) 7309–7318.
[40] R.A. Mathias, J.W. Lim, H. Ji, R.J. Simpson, Methods Mol. Biol. 528 (2009) 227–242.
[41] M. Lenassi, G. Cagney, M. Liao, T. Vaupotic, K. Bartholomeeusen, Y. Cheng, N.J. Krogan, A. Plemenitas, B.M. Peterlin, Traffic 11 (2010) 110–122.
[42] M. Kovacsovics-Bankowski, K. Clark, B. Benacerraf, K.L. Rock, Proc. Natl. Acad. Sci. USA 90 (1993) 4942–4946.
[43] C. Thery, S. Amigorena, G. Raposo, A. Clayton. Curr. Protoc. Cell Biol. Chapter 3 (2006) Unit 3, 22.
[44] H.G. Lamparski, A. Metha-Damani, J.Y. Yao, S. Patel, D.H. Hsu, C. Ruegg, J.B. Le Pecq, J. Immunol. Methods 270 (2002) 211–226.
[45] R. Cantin, J. Diou, D. Belanger, A.M. Tremblay, C. Gilbert, J. Immunol. Methods 338 (2008) 21–30.
[46] A. Clayton, J. Court, H. Navabi, M. Adams, M.D. Mason, J.A. Hobot, G.R. Newman, B. Jasani, J. Immunol. Methods 247 (2001) 163–174.
[47] K. Koga, K. Matsumoto, T. Akiyoshi, M. Kubo, N. Yamanaka, A. Tasaki, H. Nakashima, M. Nakamura, S. Kuroki, M. Tanaka, M. Katano, Anticancer Res. 25 (2005) 3703–3707.
[48] S. Mathivanan, J.W. Lim, B.J. Tauro, H. Ji, R.L. Moritz, R.J. Simpson, Mol. Cell. Proteomics 9 (2010) 197–208.
[49] R.H. Whitehead, J.K. Jones, A. Gabriel, R.E. Lukies, Cancer Res. 47 (1987) 2683–2689.
[50] T.H. Steinberg, W.M. Lauber, K. Berggren, C. Kemper, S. Yue, W.F. Patton, Electrophoresis 21 (2000) 497–508.
[51] M. Schroder, R. Schafer, P. Friedl, Anal. Biochem. 244 (1997) 174–176.
[52] R.J. Simpson, L.M. Connolly, J.S. Eddes, J.J. Pereira, R.L. Moritz, G.E. Reid, Electrophoresis 21 (2000) 1707–1732.
[53] D.W. Greening, R.J. Simpson, J. Proteomics 73 (2010) 637–648.
[54] J.V. Olsen, L.M. de Godoy, G. Li, B. Macek, P. Mortensen, R. Pesch, A. Makarov, O. Lange, S. Horning, M. Mann, Mol. Cell. Proteomics 4 (2005) 2010–2021.
[55] K.D. Pruitt, T. Tatusova, D.R. Maglott, Nucleic Acids Res. 35 (2007) D61–D65.
[56] D.N. Perkins, D.J. Pappin, D.M. Creasy, J.S. Cottrell, Electrophoresis 20 (1999) 3551–3567.
[57] D.W. Greening, K.M. Glenister, E.A. Kapp, R.L. Moritz, R.L. Sparrow, G.W. Lynch, R.J. Simpson, Proteomics Clin. Appl. 2 (2008) 63–77.
[58] G.R. Mishra, M. Suresh, K. Kumaran, N. Kannabiran, S. Suresh, P. Bala, K. Shivakumar, N. Anuradha, R. Reddy, T.M. Raghavan, S. Menon, G. Hanumanthu, M. Gupta, S. Upendran, S. Gupta, M. Mahesh, B. Jacob, P. Mathew, P. Chatterjee, K.S. Arun, S. Sharma, K.N. Chandrika, N. Deshpande, K. Palvankar, R. Raghavnath, R. Krishnakanth, H. Karathia, B. Rekha, R. Nayak, G. Vishnupriya, H.G. Kumar, M. Nagini, G.S. Kumar, R. Jose, P. Deepthi, S.S. Mohan, T.K. Gandhi, H.C. Harsha, K.S. Deshpande, M. Sarker, T.S. Prasad, A. Pandey, Nucleic Acids Res. 34 (2006) D411–D414.
[59] I. Letunic, T. Doerks, P. Bork, Nucleic Acids Res. 37 (2009) D229–D232.
[60] E.L. Sonnhammer, G. von Heijne, A. Krogh, Proc. Int. Conf. Intell. Syst. Mol. Biol. 6 (1998) 175–182.
[61] S. Mathivanan, R.J. Simpson, Proteomics 9 (2009) 4997–5000.
[62] S. Mathivanan, C.J. Fahner, G.E. Reid, R.J. Simpson, Nucleic Acids Res. 40 (2012) D1241–D1244.
[63] Y.S. Chen, R.A. Mathias, S. Mathivanan, E.A. Kapp, R.L. Moritz, H.J. Zhu, R.J. Simpson, Mol. Cell. Proteomics 10 (2011) M110. 001131.
[64] T. Beissbarth, L. Hyde, G.K. Smyth, C. Job, W.M. Boon, S.S. Tan, H.S. Scott, T.P. Speed, Bioinformatics 20 (Suppl. 1) (2004) i31–i39.
[65] W.M. Old, K. Meyer-Arendt, L. Aveline-Wolf, K.G. Pierce, A. Mendoza, J.R. Sevinsky, K.A. Resing, N.G. Ahn, Mol. Cell. Proteomics 4 (2005) 1487–1502.
[66] H. Stenmark, Nat. Rev. Mol. Cell Biol. 10 (2009) 513–525.
[67] T. Abache, F. Le Naour, S. Planchon, F. Harper, C. Boucheix, E. Rubinstein, J. Cell. Biochem. 102 (2007) 650–664.
[68] R. Jahn, R.H. Scheller, Nat. Rev. Mol. Cell Biol. 7 (2006) 631–643.
[69] E. Vincan, T. Brabletz, M.C. Faux, R.G. Ramsay, Cells Tissues Organs 185 (2007) 20–28.
[70] V. Sokolova, A.K. Ludwig, S. Hornung, O. Rotan, P.A. Horn, M. Epple, B. Giebel, Colloids Surf. B Biointerfaces 87 (2010) 146–150.
[71] A. van Zon, M.H. Mossink, R.J. Scheper, P. Sonneveld, E.A. Wiemer, Cell. Mol. Life Sci. 60 (2003) 1828–1837.
[72] Y. Xie, J. Mol. Cell. Biol. 2 (2010) 308–317.
[73] S. Smith, FASEB J. 8 (1994) 1248–1259.
[74] G. Odorizzi, J. Cell Sci. 119 (2006) 3025–3032.
[75] L.V. Coren, T. Shatzer, D.E. Ott, Retrovirology 5 (2008) 64.
[76] D. Maetzel, S. Denzel, B. Mack, M. Canis, P. Went, M. Benk, C. Kieu, P. Papior, P.A. Baeuerle, M. Munz, O. Gires, Nat. Cell Biol. 11 (2009) 162–171.
[77] M. Trzpis, P.M. McLaughlin, L.M. de Leij, M.C. Harmsen, Am. J. Pathol. 171 (2007) 386–395.
[78] S. Sawamiphak, S. Seidel, C.L. Essmann, G.A. Wilkinson, M.E. Pitulescu, T. Acker, A. Acker-Palmer, Nature 465 (2010) 487–491.
[79] G. van Niel, I. Porto-Carreiro, S. Simoes, G. Raposo, J. Biochem. 140 (2006) 13–21.
[80] C. Raiborg, H. Stenmark, Nature 458 (2009) 445–452.
[81] M. Fukuda, Cell. Mol. Life Sci. 65 (2008) 2801–2813.
[82] M. Wilcke, L. Johannes, T. Galli, V. Mayau, B. Goud, J. Salamero, J. Cell Biol. 151 (2000) 1207–1220.
[83] A. Savina, M. Vidal, M.I. Colombo, J. Cell Sci. 115 (2002) 2505–2515.
[84] C. Hsu, Y. Morohashi, S. Yoshimura, N. Manrique-Hoyos, S. Jung, M.A. Lauterbach, M. Bakhti, M. Gronborg, W. Mobius, J. Rhee, F.A. Barr, M. Simons, J. Cell Biol. 189 (2010) 223–232.
[85] M. Ostrowski, N.B. Carmo, S. Krumeich, I. Fanget, G. Raposo, A. Savina, C.F. Moita, K. Schauer, A.N. Hume, R.P. Freitas, B. Goud, P. Benaroch, N. Hacohen, M. Fukuda, C. Desnos, M.C. Seabra, F. Darchen, S. Amigorena, L.F. Moita, C. Thery, Nat. Cell Biol. 12 (2010) 19–30; pp. 1–13.
[86] A. de Gassart, C. Geminard, D. Hoekstra, M. Vidal, Traffic 5 (2004) 896–903.
[87] C. D'Souza-Schorey, G. Li, M.I. Colombo, P.D. Stahl, Science 267 (1995) 1175–1178.
[88] D.J. Yamashiro, B. Tycko, S.R. Fluss, F.R. Maxfield, Cell 37 (1984) 789–800.
[89] A.O. Johnson, R.N. Ghosh, K.W. Dunn, R. Garippa, J. Park, S. Mayor, F.R. Maxfield, T.E. McGraw, J. Cell Biol. 135 (1996) 1749–1762.
[90] J.M. Beekman, P.J. Coffer, J. Cell Sci. 121 (2008) 1349–1355.
[91] W. Hong, Biochim. Biophys. Acta 1744 (2005) 493–517.
[92] N. Hasan, C. Hu, Exp. Cell Res. 316 (2010) 12–23.
[93] C. Claas, C.S. Stipp, M.E. Hemler, J. Biol. Chem. 276 (2001) 7974–7984.
[94] I. Nazarenko, S. Rana, A. Baumann, J. McAlear, A. Hellwig, M. Trendelenburg, G. Lochnit, K.T. Preissner, M. Zoller, Cancer Res. 70 (2010) 1668–1678.
[95] A. Lakkaraju, E. Rodriguez-Boulan, Trends Cell Biol. 18 (2008) 199–209.
[96] M. Miyanishi, K. Tada, M. Koike, Y. Uchiyama, T. Kitamura, S. Nagata, Nature 450 (2007) 435–439.
[97] E.N. Nolte-'t Hoen, S.I. Buschow, S.M. Anderton, W. Stoorvogel, M.H. Wauben, Blood 113 (2009) 1977–1981.
[98] E. Segura, C. Nicco, B. Lombard, P. Veron, G. Raposo, F. Batteux, S. Amigorena, C. Thery, Blood 106 (2005) 216–223.
[99] S. Rana, C. Claas, C.C. Kretz, I. Nazarenko, M. Zoeller, Int. J. Biochem. Cell Biol. 43 (2011) 106–119.
[100] K.N. Pandey, Front Biosci. 14 (2009) 5339–5360.
[101] S. Shah, S.F. Lee, K. Tabuchi, Y.H. Hao, C. Yu, Q. LaPlant, H. Ball, C.E. Dann 3rd, T. Sudhof, G. Yu, Cell 122 (2005) 435–447.
[102] J.A. Cho, D.J. Yeo, H.Y. Son, H.W. Kim, D.S. Jung, J.K. Ko, J.S. Koh, Y.N. Kim, C.W. Kim, Int. J. Cancer 114 (2005) 613–622.
[103] T. Jung, D. Castellana, P. Klingbeil, I. Cuesta Hernandez, M. Vitacolonna, D.J. Orlicky, S.R. Roffler, P. Brodt, M. Zoller, Neoplasia 11 (2009) 1093–1105.

[104] B. Busser, L. Sancey, E. Brambilla, J.L. Coll, A. Hurbin, Biochim. Biophys. Acta 1816 (2011) 119–131.
[105] H. Surawska, P.C. Ma, R. Salgia, Cytokine Growth Factor Rev. 15 (2004) 419–433.
[106] N.I. Herath, A.W. Boyd, Int. J. Cancer 126 (2010) 2003–2011.
[107] T. Mahmoudi, V.S. Li, S.S. Ng, N. Taouatas, R.G. Vries, S. Mohammed, A.J. Heck, H. Clevers, EMBO J. 28 (2009) 3329–3340.
[108] P. Polakis, Genes Dev. 14 (2000) 1837–1851.
[109] J.A. Thompson, F. Grunert, W. Zimmermann, J. Clin. Lab. Anal. 5 (1991) 344–366.
[110] J. Hashino, Y. Fukuda, S. Oikawa, H. Nakazato, T. Nakanishi, Clin. Exp. Metastasis 12 (1994) 324–328.
[111] A. Clayton, C.L. Harris, J. Court, M.D. Mason, B.P. Morgan, Eur. J. Immunol. 33 (2003) 522–531.